Available online at www.sciencedirect.com
SCIENCE DIRECT®
PERGAMON
International Journal of Heat and Mass Transfer 46 (2003) 1075–1083
International Journal of HEAT and MASS TRANSFER
www.elsevier.com/locate/ijhmt

Natural convection heat and mass transfer along a vertical wavy surface

Jer-Huan Jang [a], Wei-Mon Yan [b,*], Hui-Chung Liu [b]

[a] Department of Mechanical Engineering, Kuang-Wu Institute of Technology, Pei-To, Taipei 112, Taiwan
[b] Graduate Institute of Mechatronic Engineering, Huafan University, Shih-Ting, Taipei 223, Taiwan

Received 17 October 2001; received in revised form 28 August 2002

Abstract

A numerical study of natural convection heat and mass transfer along a vertical wavy surface has been performed. The wavy surface is maintained at uniform wall temperature and constant wall concentration. A simple coordinate transformation is employed to transform the complex wavy surface to a flat plate. A marching finite-difference scheme is used for the analysis. The buoyancy ratio N, amplitude–wavelength ratio α, and Schmidt number Sc are important parameters for this problem. The numerical results, including the developments of skin-friction coefficient, velocity, temperature, concentration, Nusselt number as well as Sherwood number along the wavy surfaces are presented. The effects of the buoyancy ratio N and the dimensionless amplitude of wavy surface on the local Nusselt number and the local Sherwood number have been examined in detail.

1. Introduction

There are many physical processes in which buoyancy forces resulting from combined thermal and species diffusion play an important role in the convective transfer of heat and mass. The engineering applications include the chemical distillatory processes, formation and dispersion of fog, design of heat exchangers, channel type solar energy collectors, and thermo-protection systems. Therefore, the characteristics of natural convection heat and mass transfer are relatively important. Convection flows driven by temperature and concentration differences have been studied extensively in the past. Bejan and Khair [1] used Darcy's law to study the features of natural convection boundary layer flow driven by temperature and concentration gradients in a porous medium. Chang et al. [2] investigated the combined buoyancy effects of thermal and mass diffusion on the natural convection flows in a vertical open tube. Yan and Lin [3] studied combined heat and mass transfer natural convection between vertical parallel plates with film evaporation.

Previous studies of natural convection heat and mass transfer have focused mainly on a flat plate or regular ducts. Somers [4], Mather et al. [5], and Gill et al. [6] analyzed the same problem of simultaneous heat transfer and binary diffusion on a vertical surface with different situations or different numerical schemes. Bottemanne [7] has considered simultaneous heat and mass transfer by free convection along a vertical flat plate only for steady state theoretical solutions with $Pr = 0.71$ and $Sc = 0.63$. Callahan and Marner [8] studied the free convection with mass transfer on a vertical flat plate with $Pr = 1$ and a realistic range of Schmidt number. The effects of mass diffusion on natural convection flows along a flat plate with different inclination have been studied rather extensively. Gebhart and Pera [9], Chen and Yuh [10] and Srinivasan and Angirasa [11] investigated the effects of inclination of flat plate on the combined heat and mass transfer in natural convection. Jang and Chang [12] studied the problem of buoyancy-induced inclined boundary flows in a porous medium resulting from combined heat and mass buoyancy effects. However, studies on the effects of complex

* Corresponding author. Tel.: +886-2-26632102x4038; fax: +886-2-2663-3847.
E-mail address: wmyan@huafan.hfu.edu.tw (W.-M. Yan).

0017-9310/03/$ - see front matter
PII: S0017-9310(02)00361-7

Nomenclature

a	amplitude of the wavy surface (m)
c	concentration
C	dimensionless concentration
C_f	skin-friction coefficient
C_p	specific heat of fluid at constant pressure ($kJ\,kg^{-1}\,K^{-1}$)
D	mass diffusivity ($m^2\,s^{-1}$)
g	gravitational acceleration ($m\,s^{-2}$)
k	conductivity ($W\,m^{-1}\,K^{-1}$)
L	wavelength of the wavy surface (m)
N	buoyancy ratio, Eq. (6)
Nu	Nusselt number
P	pressure ($N\,m^{-2}$)
Pr	Prandtl number
Sc	Schmidt number
Sh	Sherwood number
T	temperature (K)
U, V	dimensionless velocity
$\widetilde{U}$	characteristic velocity
u, v	velocity components in the x and y directions, respectively ($m\,s^{-1}$)
X, Y	dimensionless coordinate system
x, y	coordinate system (m)

Greek symbols

α	amplitude–wavelength ratio, a/L
β_T	thermal expansion coefficient
β_c	concentration expansion coefficient
σ	dimensionless coordinate of the wavy surface
$\overline{\sigma}$	coordinate of the wavy surface, Eq. (1)
μ	viscosity ($kg\,m^{-1}\,s^{-1}$)
ρ	fluid density ($kg\,m^{-3}$)
θ	dimensionless temperature

Superscript

$*$	non-dimensional quantity

Subscripts

∞	conditions far away from the surface
c	caused by concentration
m	mean value
T	caused by temperature
w	surface condition
x	local value

geometries on the natural convection heat and mass transfer are still required in this area. Few studies have considered the effects of complex geometries on thermal convection in micropolar fluids, including the flows along a convex surface. Wang and Kleinstreuer [13] investigated the thermal convection on micropolar fluids passing a convex with suction/injection. Yih [14] studied the heat and mass transfer characteristic in natural convection flow over a truncated cone subjected to uniform wall temperature and concentration or uniform heat and mass flux embedded in porous media. Wu et al. [15] developed a numerical model to study the effectiveness of dehydration media for wedge-shaped surface with mass and heat transfer.

It is necessary to study the heat and mass transfer from an irregular surface because irregular surfaces are often present in many applications. It is often encountered in heat transfer devices to enhance heat transfer. For examples, flat-plate solar collectors and flat-plate condensers in refrigerators. The natural convection heat transfer from an isothermal vertical wavy surface was first studied by Yao [16–18] and using an extended Prantdl's transposition theorem and a finite-difference scheme. He proposed a simple transformation to study the natural convection heat transfer from isothermal vertical wavy surfaces, such as sinusoidal surface. Chiu and Chou [19] studied the natural convection heat transfer along a vertical wavy surface in micropolar fluids. Chen and Wang [20,21] analyzed transient forced and free convection along a wavy surface in microfluids. Cheng [22,23] has investigated coupled heat and mass transfer by natural convection flow along a wavy conical surface and vertical wavy surface in a porous medium.

Most of the previous studies about vertical wavy surfaces are concerned with microfluids or porous media. Natural convection heat and mass transfer in Newtonian fluid along a vertical wavy surface has not been well investigated. The objective of this study is to examine numerically the natural convection heat and mass transfer along a vertical wavy surface by using Prandtl's transposition theorem and to investigate the effect of irregular surfaces on the characteristics of natural convection heat and mass transfer. The numerical results, including the developments of friction factor, velocity, temperature, concentration, Nusselt number as well as Sherwood number along the wavy surface are presented. The effects of the buoyancy ratio N and the dimensionless amplitude of wavy surface on the local Nusselt number and the local Sherwood number are also studied in detail.

2. Analysis

Consider a semi-infinite vertical wavy plate as shown schematically in Fig. 1. The wavy surface of the plate can be described by

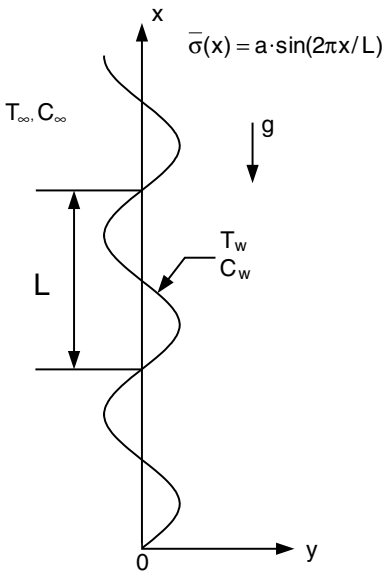

Fig. 1. Schematic diagram of the physical system.

$$y = \overline{\sigma}(x) = a\sin(2\pi x/L)$$

where a is the amplitude of the wavy surface and L is the characteristic wavelength of the wavy surface. The origin of the coordinate system is placed at the leading edge of the vertical surface. The surface is kept at uniform temperature T_w and uniform concentration c_w. The u and v are the velocity components in the x and y directions, respectively. The fluid oncoming to the surface has a constant temperature T_∞ and concentration c_∞. The flow is assumed to be steady and the thermal properties of the mixture are assumed to be constant except for the density variation in the buoyancy term of the transverse-momentum equation.

The governing equations for a steady, laminar, and incompressible flow along a semi-infinite vertical wavy surface with Boussinesq approximation may be written as:

Continuity equation

$$\frac{\partial u}{\partial x} + \frac{\partial v}{\partial y} = 0 \tag{1}$$

Momentum equation

$$\rho\left(u\frac{\partial u}{\partial x} + v\frac{\partial u}{\partial y}\right) = -\frac{\partial P}{\partial x} + \mu\left(\frac{\partial^2 u}{\partial x^2} + \frac{\partial^2 u}{\partial y^2}\right) + \rho g\beta_T(T - T_\infty) + \rho g\beta_c(c - c_\infty) \tag{2}$$

$$\rho\left(u\frac{\partial v}{\partial x} + v\frac{\partial v}{\partial y}\right) = -\frac{\partial P}{\partial y} + \mu\left(\frac{\partial^2 v}{\partial x^2} + \frac{\partial^2 v}{\partial y^2}\right) \tag{3}$$

Energy equation

$$\rho C_p\left(u\frac{\partial T}{\partial x} + v\frac{\partial T}{\partial y}\right) = k\left(\frac{\partial^2 T}{\partial x^2} + \frac{\partial^2 T}{\partial y^2}\right) \tag{4}$$

Concentration equation

$$u\frac{\partial c}{\partial x} + v\frac{\partial c}{\partial y} = D\left(\frac{\partial^2 c}{\partial x^2} + \frac{\partial^2 c}{\partial y^2}\right) \tag{5}$$

Moreover, the appropriate boundary conditions for the problem are: at the wavy surface, $u = 0$, $v = 0$, $T = T_w$, $c = c_w$; matching with the quiescent free stream, $u = 0$, $v = 0$, $T = T_\infty$, $c = c_\infty$.

In non-dimensionalizing the governing equations, the following dimensionless variables were introduced

$$x^* = \frac{x}{L}; \quad y^* = \frac{y - \overline{\sigma}}{L}Gr^{1/4}; \quad u^* = \frac{\rho L}{\mu Gr^{1/2}}u;$$
$$v^* = \frac{\rho L}{\mu Gr^{1/4}}(v - \sigma' u); \quad P^* = \frac{\rho L^2}{\mu^2 Gr}P;$$
$$Gr = \frac{g\beta_T(T_w - T_\infty)\rho^2 L^3}{\mu^2}; \quad Pr = \frac{\mu C_p}{K}; \quad Sc = \frac{\mu}{\rho D};$$
$$\theta = \frac{T - T_\infty}{T_w - T_\infty}; \quad C = \frac{c - c_\infty}{c_w - c_\infty}; \quad N = \frac{\beta_c(c_w - c_\infty)}{\beta_T(T_w - T_\infty)};$$
$$\sigma = \frac{\overline{\sigma}}{L} \tag{6}$$

It is noted that when N is equal to zero, there is no mass diffusion body force and the problem reduces to pure heat convection; when N becomes infinite, there is no thermal diffusion.

After ignoring the small order terms in Gr, the dimensionless governing equations become

$$\frac{\partial u^*}{\partial x^*} + \frac{\partial v^*}{\partial y^*} = 0 \tag{7}$$

$$u^*\frac{\partial u^*}{\partial x^*} + v^*\frac{\partial u^*}{\partial y^*} = -\frac{\partial P^*}{\partial x^*} + \sigma'\frac{\partial P^*}{\partial y^*}Gr^{1/4} + (1 + \sigma'^2) \times \frac{\partial^2 u^*}{\partial y^{*2}} + \theta + NC \tag{8}$$

$$u^{*2}\sigma'' + \sigma'(\theta + NC) = \sigma'\frac{\partial P^*}{\partial x^*} - (1 + \sigma'^2)\frac{\partial P^*}{\partial y^*}Gr^{1/4} \tag{9}$$

$$u^*\frac{\partial \theta}{\partial x^*} + v^*\frac{\partial \theta}{\partial y^*} = \frac{1}{Pr}(1 + \sigma'^2)\frac{\partial^2 \theta}{\partial y^{*2}} \tag{10}$$

$$u^*\frac{\partial C}{\partial x^*} + v^*\frac{\partial C}{\partial y^*} = \frac{1}{Sc}(1 + \sigma'^2)\frac{\partial^2 C}{\partial y^{*2}} \tag{11}$$

It is worth noting that the σ' and σ'' indicate the first and second differentiations of σ with respect to x. Eq. (8) shows that when $N < 0$, the mass diffusion buoyancy forces oppose those of thermal diffusion, and when $N > 0$, the mass diffusion buoyancy forces aid those of thermal diffusion.

For the current problem, the pressure gradient $\partial P^*/\partial x^*$ is zero. Therefore, eliminating $\partial P^*/\partial y^*$ in Eqs. (8) and (9) resulting the following equation:

$$u^*\frac{\partial u^*}{\partial x^*}+v^*\frac{\partial u^*}{\partial y^*}=\frac{1}{1+\sigma'^2}(\theta+NC-u^{*2}\sigma'\sigma'')+(1+\sigma'^2)\frac{\partial^2 u^*}{\partial y^{*2}} \tag{12}$$

Use the following transformation in order to remove the singularity at the leading edge [16]:

$$X=x^*;\quad Y=\frac{y^*}{(4x^*)^{1/4}};\quad U=\frac{u^*}{(4x^*)^{1/2}};\quad V=(4x^*)^{1/4}v^* \tag{13}$$

then Eqs. (7) and (10)–(12) in the parabolic coordinates (X,Y) become

$$2U+4X\frac{\partial U}{\partial X}-Y\frac{\partial U}{\partial Y}+\frac{\partial V}{\partial Y}=0 \tag{14}$$

$$4XU\frac{\partial U}{\partial X}+(V-UY)\frac{\partial U}{\partial Y}+\left(2+\frac{4X\sigma'\sigma''}{1+\sigma'^2}\right)U^2=\frac{1}{1+\sigma'^2}(\theta+NC)+(1+\sigma'^2)\frac{\partial^2 U}{\partial Y^2} \tag{15}$$

$$4XU\frac{\partial \theta}{\partial X}+(V-UY)\frac{\partial \theta}{\partial Y}=\frac{1}{Pr}(1+\sigma'^2)\frac{\partial^2\theta}{\partial Y^2} \tag{16}$$

$$4XU\frac{\partial C}{\partial X}+(V-UY)\frac{\partial C}{\partial Y}=\frac{1}{Sc}(1+\sigma'^2)\frac{\partial^2 C}{\partial Y^2} \tag{17}$$

The corresponding boundary conditions are

$$Y=0;\quad U=V=0;\quad \theta=1;\quad C=1 \tag{18}$$

$$Y\to\infty;\quad U\to 0;\quad \theta\to 0;\quad C\to 0 \tag{19}$$

After obtaining the velocity, temperature and concentration fields along the wavy surface, the computations of the local friction coefficient, Nusselt number, and Sherwood number are of practical interest. The local heat and mass transfer rates are large when the normal velocity is approaching the surface; they are small when the convective stream moves away from the surface. The heat and mass transfer mechanism along a wavy surface is different from that along a flat surface, and is modified by the fluid motion normal to the surface.

The local Nusselt number and Sherwood number are defined respectively as

$$Nu_x=\frac{hx}{k}=-\left(\frac{Gr}{4X}\right)^{1/4}(1+\sigma'^2)^{1/2}\left(\frac{\partial\theta}{\partial Y}\right)_{Y=0} \tag{20}$$

$$Sh_x=\frac{h_D x}{D}=-\left(\frac{Gr}{4X}\right)^{1/4}(1+\sigma'^2)^{1/2}\left(\frac{\partial C}{\partial Y}\right)_{Y=0} \tag{21}$$

The shearing stress on the wavy surface is

$$\tau_w=\left[\mu\left(\frac{\partial u}{\partial y}+\frac{\partial v}{\partial x}\right)\right]_{y=0} \tag{22}$$

Since the local skin-friction coefficient C_{fx} is defined by

$$C_{fx}=\frac{2\tau_w}{\rho\widetilde{U}^2} \tag{23}$$

where $\widetilde{U}=(\mu Gr^{1/2})/(\rho L)$ is a characteristic velocity. Substituting Eq. (22) into Eq. (23) in terms of the non-dimensional quantities, we have

$$C_{fx}=\left(\frac{4X}{Gr}\right)^{1/4}2(1-\sigma'^2)\left(\frac{\partial U}{\partial Y}\right)_{Y=0} \tag{24}$$

3. Numerical approach

In this work, a marching finite-difference scheme was used to solve the coupled governing equations for U, V, θ and C. In the transverse direction (Y), 251 non-uniform grid points were employed. Some of the calculations were tested using 501 grid points in the Y direction, but no significant improvement over the 251 grid points was found. Additionally, there are 401 grid points in the marching direction. In the program test, a finer axial step size was tried and found to give acceptable accuracy. In writing the finite-difference equations, a fully implicit numerical scheme in which the axial convection is approximated by the upstream difference and the transverse convection and diffusion terms by the central difference is used to transform the governing equations into the finite-difference equations. Each of the finite-difference equations forms a tridiagonal matrix equation, which can be efficiently solved by the Thomas algorithm [24]. During the program test, the convergent criteria for the relative errors of the variables, U, V, θ and C, between two iterations are less 10^{-5}. To further check the adequacy of the numerical scheme used in this work, the results for the limiting case of natural convection heat transfer in a wavy surface were first obtained. Excellent agreement between the present predictions and those of Yao [16] was found. Through these program tests, it was found that the present numerical method is suitable for this study.

4. Results and discussion

In the present study, numerical calculations are performed for the wavy surface described by $\overline{\sigma}(x)=a\sin(2\pi x/L)$ or dimensionless $\sigma(X)=\alpha\sin(2\pi X)$ for amplitude–wavelength ratio of 0–0.1. In this work, the air mixture with various mass species is considered. Additionally, only the results of Schmidt number ranging from 0.2 to 2 are presented. The velocity distribution along X-axis of this study is presented in Fig. 2. The

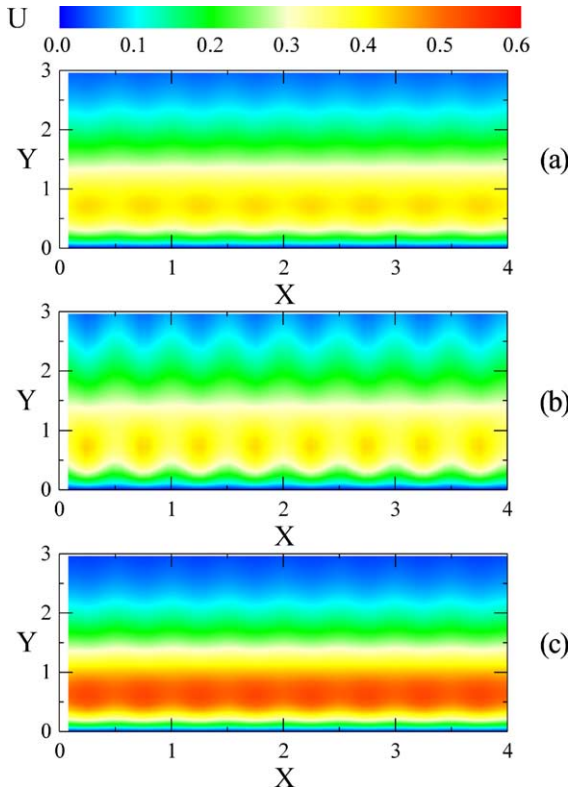

Fig. 2. The velocity contours: (a) $\alpha = 0.05$, $N = 2$, $Sc = 1.3$; (b) $\alpha = 0.1$, $N = 2$, $Sc = 1.3$; (c) $\alpha = 0.1$, $N = 4$, $Sc = 1.3$.

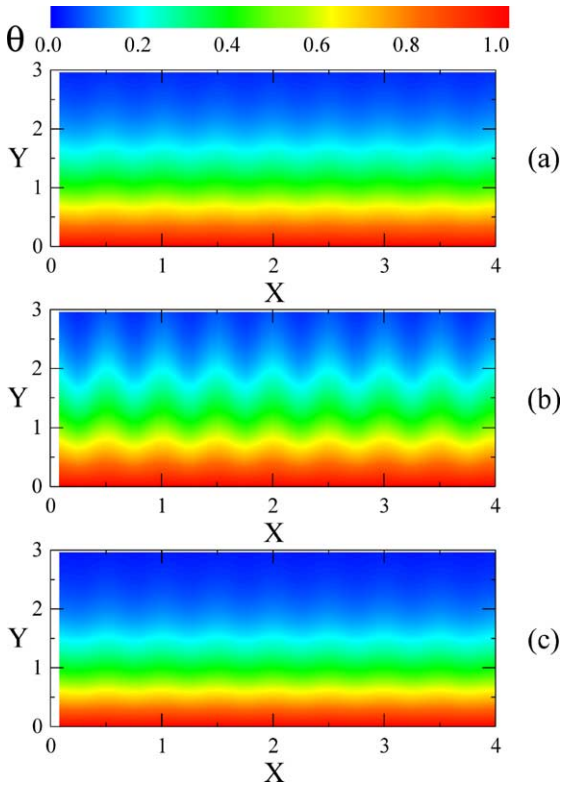

Fig. 3. The temperature contours: (a) $\alpha = 0.05$, $N = 2$, $Sc = 1.3$; (b) $\alpha = 0.1$, $N = 2$, $Sc = 1.3$; (c) $\alpha = 0.1$, $N = 4$, $Sc = 1.3$.

temperature and concentration distributions are obtained and shown in Figs. 3 and 4 respectively as well. In these figures, there are three different cases for numerical calculation, where (a) represents the typical case, and the values of α, N, and Sc are 0.05, 2, and 1.3, respectively; (b) represents the case of $\alpha = 0.1$, $N = 2$, and $Sc = 1.3$; and (c) represents the case of $\alpha = 0.1$, $N = 4$, $Sc = 1.3$. Because the leading edge of the wavy surface is a singular point, the results near this particular position are not presented in these figures.

The nodes of the wavy surface are at $X = 0.5$, 1, 1.5, 2, etc. and while $X = 0.75$, 1.75, 2.75 and so on are the troughs, and $X = 0.25$, 1.25, 2.25 etc. are the crests. It is observed that the developments of velocity, temperature and concentration profiles change periodically along the X-axis in Figs. 2–4. It is interesting to see that the wavelengths of wavy velocity, temperature and concentration distributions are the same and are exactly the half wavelength of the wavy surface. That is, a maximum occurs on the nodes of the wavy surface. From Eqs. (14)–(17), the coefficient of higher order differential terms contains σ'^2. Since σ is a periodical function with wavelength of l, σ'^2 is also a periodical function with wavelength of $l/2$. Therefore, the solution of Eqs. (14)–(17) becomes a periodical function with wavelength of $l/2$. This could be used to explain the physical phenomena mentioned above.

In Fig. 2, the hydrodynamic boundary layer and the maximum velocity value are about the same and there occurs a periodical phenomenon for these three cases. It is obvious that the boundary layers are thicker near the nodes than those near the crests and the troughs. But the maximum velocity in the crests or the troughs is larger than that on the nodes. There is a greater velocity fluctuation for a higher amplitude–wavelength ratio α by comparing cases (a) and (b). When the buoyancy ratio N increases, the maximum velocity increases by comparing cases (b) and (c). Obviously, the contribution of mass diffusion to the buoyancy force increases significantly the maximum velocity.

In Figs. 3 and 4, the developments of temperature and concentration profiles are similar. This is due to the fact that the temperature and concentration governing equations are similar and the only difference between them is the Prantdl number Pr of the energy equation from the Schmidt number Sc of the species equation. Comparison of Figs. 3 and 4 indicates that the thermal boundary layers are thicker than those of concentration for these three cases. This is because that the Schmidt

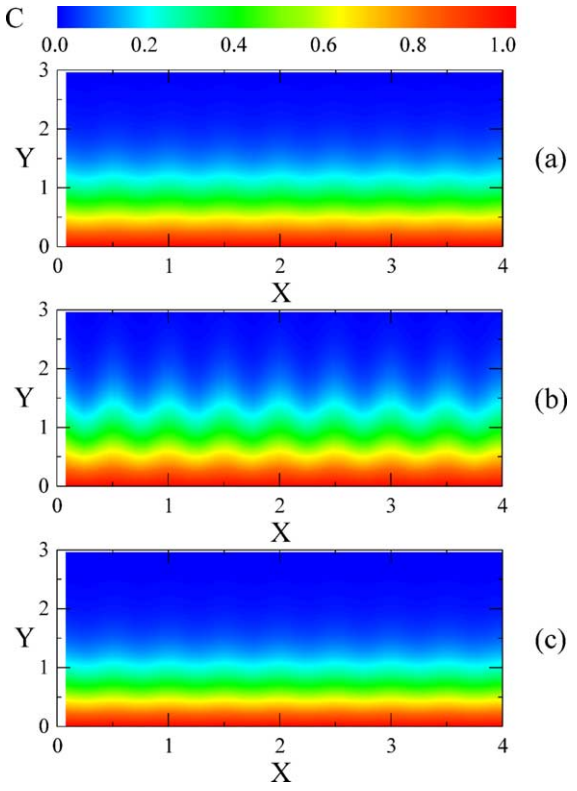

Fig. 4. The concentration contours: (a) $\alpha = 0.05$, $N = 2$, $Sc = 1.3$; (b) $\alpha = 0.1$, $N = 2$, $Sc = 1.3$; (c) $\alpha = 0.05$, $N = 4$, $Sc = 1.3$.

number Sc ($=1.3$) is greater than Prandtl number Pr ($=0.7$). In Fig. 3, the thermal boundary layer is thicker in case (b) comparing with case (c). The decrease of thermal boundary layer is caused by increasing the buoyancy ratio N.

Fig. 5 shows the geometric effect on local skin-friction coefficient C_{fx}, local Nusselt number Nu_x, and local Sherwood number Sh_x. It is observed that when the amplitude–wavelength ratio α increases for a fixed location of X-axis, the skin-friction coefficient, local Nusselt number and local Sherwood number decreases with greater fluctuating amplitudes. Therefore, the heat and mass transfer rates decrease as the amplitude–wavelength ratio increases. But the skin-friction coefficients on the crests and the troughs keep the same value as that on a flat plate, i.e., $\alpha = 0$. It can be understood that the definition of skin-friction coefficient is the velocity derivative on the surface, and the derivative on the crests and the troughs is equal to zero which is the same as that of a flat plate. Therefore, the skin-friction coefficients on the crests and the troughs are the same as that of a flat plate. When the amplitude–wavelength ratio is kept fixed, the skin-friction coefficient has a minimum on the nodes (e.g., $X = 0.5$, 1, 1.5, 2, etc.). The same phenomenon occurs for the local Nusselt number and the local Sherwood number.

Fig. 6 gives the effects of buoyancy ratio N on the local skin-friction coefficient, local Nusselt number and local Sherwood number respectively along the X-axis. It

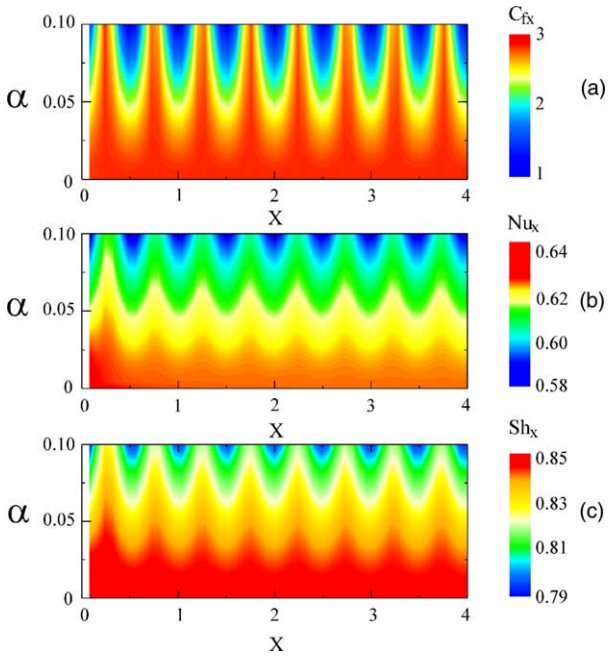

Fig. 5. Effects of amplitude–wavelength ratio α on the axial distributions of (a) skin-friction coefficient; (b) Nusselt number; (c) Sherwood number.

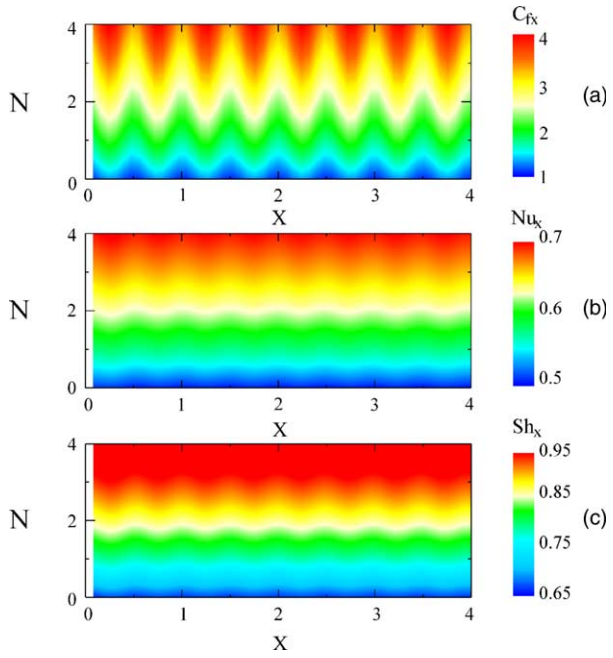

Fig. 6. Effects of buoyancy ratio N on the axial distributions of (a) skin-friction coefficient; (b) Nusselt number; (c) Sherwood number.

is obvious that when the buoyancy ratio N increases, the skin-friction coefficient, local Nusselt number, and local Sherwood number increase at a given X position. It means that the buoyancy ratio enhances the heat and mass transfer of the wavy surface. It is also worth noting that the maximum values of C_{fx}, Nu_x and Sh_x occur on

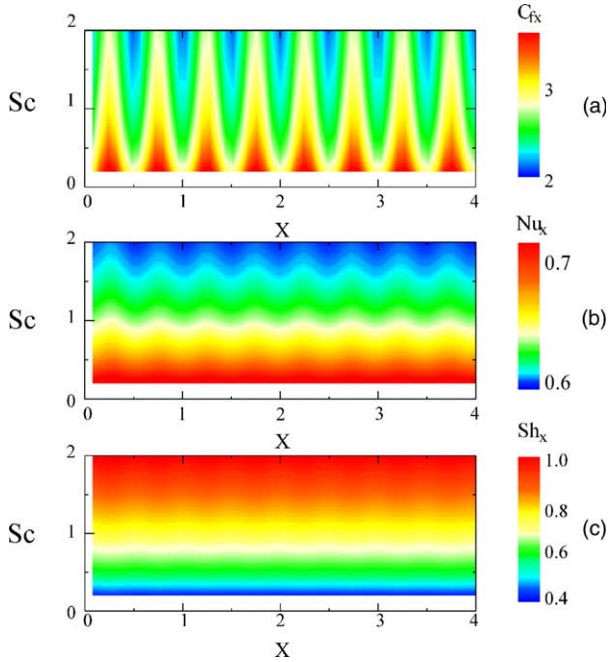

Fig. 7. Effects of Schmidt number Sc on the axial distributions of (a) skin-friction coefficient; (b) Nusselt number; (c) Sherwood number.

the nodes of the wavy surface while the minimum values occur on the crests and the troughs.

Fig. 7 illustrates the influence of Schmidt number Sc on the local skin-friction coefficient, local Nusselt number, and local Sherwood number. It is seen that the skin-friction coefficient and local Nusselt number decrease and local Sherwood number increases as Schmidt number is raised. That is, the mass transfer rate increases and the heat transfer rate decreases with increasing Schmidt number. This is due to the fact that a large Schmidt number is associated with a thinner concentration boundary layer relative to the thermal boundary layer thickness, thereby resulting in a larger concentration gradient at the wall, which in turn enhances the mass transfer.

5. Conclusions

The problem of natural convection heat and mass transfer along a wavy surface has been analyzed. The effects of amplitude–wavelength ratio α, buoyancy ratio N, and Schmidt number Sc on momentum and heat and mass transfer have been studied in detail. Brief summaries of the major results are listed in the following:

1. The properties of the flow field change periodically, and the wavelength of the properties is half of the wavelength of the wavy surface.
2. The higher amplitude–wavelength ratio α increases the fluctuation of velocity, temperature and concentration fields. However, the local skin-friction C_{fx}, Nusselt number Nu_x and Sherwood number Sh_x are smaller for larger amplitude–wavelength ratios.
3. The skin-friction coefficient, Nusselt number, and Sherwood number increase with an increase in the buoyancy ratio N. This implies that the heat and mass transfer rates increase with the buoyancy ratio.
4. Increasing Schmidt number Sc decreases the skin-friction coefficient and local Nusselt number but increases local Sherwood number. In other words, the heat transfer rate is reduced while the mass transfer rate is enhanced as the Schmidt number is raised.

Acknowledgements

The authors would like to acknowledge the financial support of the present work by the National Science Council, R.O.C. through the contract NSC89-2212-E211-016.

References

[1] A. Bejan, K.R. Khair, Heat and mass transfer by natural convection in a porous media, Int. J. Heat Mass Transfer 28 (1985) 909–918.

[2] C.J. Chang, T.F. Lin, W.M. Yan, Natural convection flows in a vertical open tube resulting from combined buoyancy effects of thermal and mass diffusion, Int. J. Heat Mass Transfer 29 (1986) 1543–1552.

[3] W.M. Yan, T.F. Lin, Combined heat and mass transfer natural convection between vertical parallel plates with film evaporation, Int. J. Heat Mass Transfer 33 (1989) 529–541.

[4] E.V. Somers, Theoretical considerations of combined thermal and mass transfer from a flat plate, ASME J. Appl. Mech. 23 (1956) 295–301.

[5] W.G. Mather, A.J. Madden, E.L. Piret, Simultaneous heat and mass transfer in free convection, Ind. Eng. Chem. 49 (1957) 961–968.

[6] W.N. Gill, E.D. Casal, D.W. Zeh, Binary diffusion and heat transfer in laminar free convection boundary layers on a vertical plate, Int. J. Heat Mass Transfer 8 (1965) 1135–1151.

[7] F.A. Bottemanne, Theoretical solution of simultaneous heat and mass transfer by free convection about a vertical flat plate, Appl. Scient. Res. 25 (1971) 137–149.

[8] G.D. Callahan, W.J. Marner, Transient free convection with mass transfer on an isothermal vertical flat plate, Int. J. Heat Mass Transfer 19 (1976) 165–174.

[9] B. Gebhart, L. Pera, The nature of vertical natural convection flows resulting from the combined buoyancy effects of thermal and mass diffusion, Int. J. Heat Mass Transfer 14 (1971) 2025–2050.

[10] T.S. Chen, C.F. Yuh, Combined heat and mass transfer in natural convection on inclined surfaces, Numer. Heat Transfer 2 (1979) 233–250.

[11] J. Srinivasan, D. Angirasa, Numerical study on double-diffusion free convection from a vertical surface, Int. J. Heat Mass Transfer 31 (1988) 2033–2038.

[12] J.Y. Jang, W.J. Chang, Buoyancy-induced inclined boundary layer flow in a saturated porous medium resulting from combined heat and mass buoyancy effects, Int. Commun. Heat Mass Transfer 15 (1988) 17–30.

[13] T.Y. Wang, C. Kleinstreuer, Thermal convection on micropolar fluids past two-dimensional or axisymmetric bodies with suction/injection, Int. J. Eng. Sci. 26 (1988) 1267–1277.

[14] K.A. Yih, Uniform transpiration effect on combined heat and mass transfer by natural convection over a cone in saturated porous media: uniform wall temperature/concentration or heat/mass flux, Int. J. Heat Mass Transfer 42 (1999) 3533–3537.

[15] C.H. Wu, D.C. Davis, J.N. Chung, L.C. Chow, Simulation of wedge-shaped product dehydration using mixtures of superheated steam and air in laminar flow, Numer. Heat Transfer 11 (1987) 109–123.

[16] L.S. Yao, Natural convection along a wavy surface, ASME J. Heat Transfer 105 (1983) 465–468.

[17] L.S. Yao, A note on Prandtl's transposition theorem, ASME J. Heat Transfer 110 (1988) 503–507.

[18] S.G. Moulic, L.S. Yao, Mixed convection along a wavy surface, ASME J. Heat Transfer 111 (1989) 974–979.

[19] C.P. Chiu, H.M. Chou, Transient analysis of natural convection along a vertical wavy surface in micropolar fluids, Int. J. Eng. Sci. 32 (1994) 19–33.

[20] C.K. Chen, C.C. Wang, Transient analysis of force convection along a wavy surface in micropolar fluids, AIAA J. Thermophys. Heat Transfer 14 (2000) 340–347.
[21] C.C. Wang, C.K. Chen, Transient force and free convection along a vertical wavy surface in micropolar fluids, Int. J. Heat Mass Transfer 44 (2001) 3241–3251.
[22] C.Y. Cheng, Natural convection heat and Mass transfer near a wavy cone with constant wall temperature and concentration in a porous medium, Mech. Res. Commun. 27 (2000) 613–620.
[23] C.Y. Cheng, Natural convection heat and mass transfer near a vertical wavy surface with constant wall temperature and concentration in a porous medium, Int. Commun. Heat Mass Transfer 27 (2000) 1143–1154.
[24] C.V. Patankar, Numerical Heat Transfer and Fluid Flow, Hemisphere/McGraw-Hill, New York, 1980.